Ogo 4 Observations of Extremely Low Frequency Hiss

J. L. R. MUZZIO[1] AND JACYNTHO J. ANGERAMI[2]

Radioscience Laboratory, Stanford University
Stanford, California 94305

An ELF hiss band with characteristics not previously identified has been observed in data from the Stanford University VLF experiment on Ogo 4. The band exhibits the typical low-frequency cutoff characteristic of downward-propagating hiss and also a peculiar upper cutoff in the vicinity of 600 Hz, which is nearly independent of the satellite altitude (~430 to 900 km) and latitude above ~15°. This band-limited ELF hiss (BLH) is observed from ~10° up to 55° dipole latitude, where the nearly constant upper cutoff and the increasing (with latitude) lower cutoff merge. Around ~10° dipole latitude, the BLH exhibits a sloping upper cutoff decreasing in frequency toward the equator (equatorial erosion). The BLH is seen most frequently from ~0600 to ~2200 LT, although some examples have been found between 0200 and 0500 LT, with less intensity. In the range 0 to 3 kHz and up to ~55° dipole latitude, the BLH is the strongest signal observed. Its peak amplitude may reach 2×10^{-4} γ^2/Hz between 40° and 50° dipole latitude during daytime (~1000 LT). After prolonged periods of low magnetic activity ($Kp \leq 2$), the upper cutoff may decrease to as low as 420 Hz but recovers about one day after a sharp increase in magnetic activity, such as a sudden commencement. The decrease and smearing of the lower cutoff of the background hiss, observed at latitudes greater than about 58°, is an indication of the light ion trough. A source location in the equatorial region near $L = 4$ was found adequate to explain the characteristics of the BLH, as well as some of the observations of ELF hiss previously reported. Two possible generation mechanisms are briefly examined (Cerenkov and Doppler-shifted cyclotron), but for either a certain amount of emission coherency or amplification is necessary to obtain the observed power fluxes.

ELF hiss or continuous noise in the range of a few hundred Hz up to about 2 or 3 kHz has been observed in the magnetosphere and reported by a number of authors [*Guthart et al.*, 1968; *Taylor and Gurnett*, 1968; *Gurnett and Burns*, 1968; *Russell et al.*, 1969; *Dunckel and Helliwell*, 1969; *Mosier*, 1971]. Their work, however, deals almost exclusively with high-latitude or high-altitude events.

In this paper, we present and discuss observations of ELF hiss using data from the Stanford University VLF experiment flown on the Ogo 4 satellite (~430- to 900-km altitude) and covering the whole range between ±84° invariant latitudes. Analysis of real-time spectrogram data acquired at the Rosman, North Carolina, and Quito and Santiago, South America, telemetry stations from September 1967 to March 1968 revealed the occurrence of a hiss band with characteristics not previously identified. The band is seen from low to medium latitudes and will be referred to as band-limited ELF hiss (BLH). Examination of several records from the telemetry stations at Johannesburg, South Africa, and Orroral, Australia, also revealed the same kind of hiss, but a more thorough analysis of data from these stations has yet to be conducted.

Furthermore, amplitude information from the digital-stepping sweeping receivers of the same experiment was gathered from 14 satellite passes extending the range to ±84° invariant latitude. However, the results and conclusions from this sample are to be considered preliminary until a more extensive study can be undertaken.

On the basis of wave-propagation properties, it is proposed that the BLH is generated at large wave normal angles in the equatorial region near $L = 4$. This model can be used to explain the characteristics of the BLH and also to interpret previous observations of ELF hiss reported by *Russell et al.* [1969] and *Mosier*

[1] Now at I.T.A., Divisão de Electrônica, Sao José dos Campos, S.P., Brazil.

[2] Now at Esc. Politécnica Univ. S. Paulo, Caixa Postal 8174, São Paulo, Brazil.

[1971]. Two mechanisms for the generation of the BLH based on radiation from energetic electrons are considered. However, in order to explain the observed intensities, some form of wave growth or a coherency mechanism has to be invoked.

OBSERVATIONS

The ELF hiss detected by Ogo 4 exhibits the typical low-frequency cutoff described by *Gurnett and Burns* [1968] and attributed to the two-ion cutoff in the dispersion relation. It also shows the following remarkable characteristics illustrated in the spectrograms of Figure 1:

1. A high-intensity hiss band is present at low to medium latitudes below ~600 Hz (BLH). Although there is hiss extending up to 2.0 or 3.0 kHz, it is not as strong or steady as the BLH, at least in the latitude range shown.
2. The upper cutoff of the BLH, in the vicinity of 600 Hz, seems to be independent of latitude and is virtually the same in both hemispheres.
3. The 'equatorial erosion' or sloping upper cutoff decreases in frequency toward the equator, near ±10° dipole latitude. It affects both the BLH and the hiss above its upper cutoff.

A similar equatorial erosion effect has been previously observed in whistlers, but, according to *Scarabucci* [1970], it is produced mainly by absorption in the lower ionosphere. There are examples of simultaneous occurrences of erosion in the BLH and in whistlers, although the frequency ranges are different. Also the BLH sometimes exhibits the erosion and the whistlers do not.

The upper and lower cutoffs of the BLH taken from the spectrograms shown in Figure 1 are plotted versus the absolute value of dipole latitude in Figure 2. Although the lower cutoff is markedly lower in the southern hemisphere (because of the lower values of local magnetic field near the South Atlantic anomaly), the upper cutoff remains essentially the same at both hemispheres.

Figure 3 depicts two other spectrograms similar to the ones in Figure 1 but recorded at higher latitudes by the Rosman telemetry station. Hiss and chorus up to ~2 kHz beyond 65° invariant latitude can be seen. On this record, the BLH is observed up to ~55° invariant latitude, where the upper and lower cutoffs merge. Above this latitude, the lower cutoff can still be seen in the background hiss until its gradual disappearance around 58° invariant

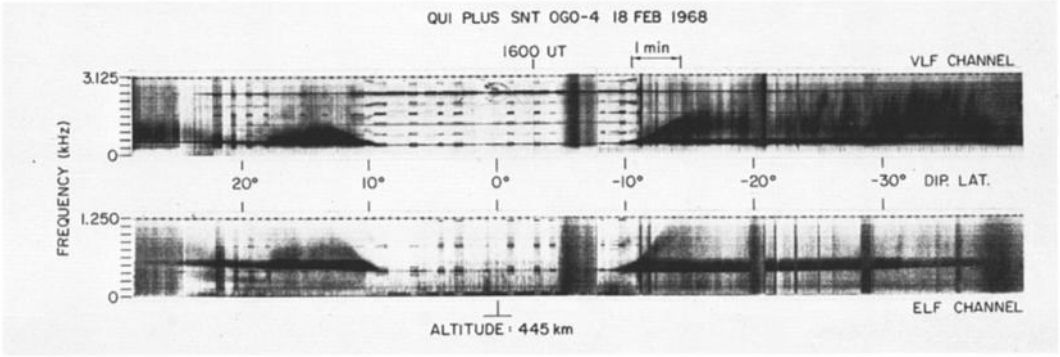

Fig. 1. Frequency versus time spectrograms of Ogo 4 ELF and VLF data recorded at Quito and Santiago, showing the ELF band-limited hiss (BLH) at the northern and southern hemispheres. The BLH is the strong hiss band below ~600 Hz. The lower panel (0–1.25 kHz) corresponds to the ELF receiver, which has a lower cutoff at ~15 Hz and a gradual upper cutoff between 300 and 1000 Hz. The upper panel (0–3.125 kHz) corresponds to a part of the VLF receiver bandwidth that covers the range 0.3–12.5 kHz. Clearly visible are the sloping upper cutoff or equatorial erosion around ±10° dipole latitude and the upper cutoff of the BLH, which is essentially independent of magnetic latitude and lies in the vicinity of 600 Hz. The lower cutoff corresponds to the familiar two-ion cutoff for downward-propagating waves. For this pass, the satellite altitude varied from 418 to 564 km. Interference lines from inverters aboard the satellite are seen at multiples of 400 Hz.

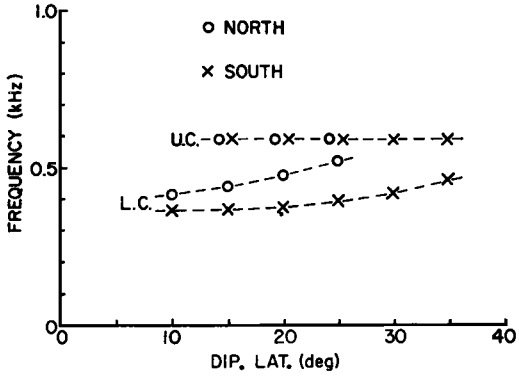

Fig. 2. Values of upper and lower cutoffs of the BLH shown in the spectrogram of Figure 1 plotted versus the modulus of dipole latitude. Although the lower cutoffs at conjugate latitudes are markedly different, mainly because of differences in the local magnetic field intensity, the upper cutoffs are essentially the same.

latitude. This disappearance of the lower cutoff is consistent with the reported decrease in the H^+ relative concentration at high latitudes [*Taylor et al.*, 1969], which causes large variations in the polarization of the wave with height and consequently greatly increases the probability of coupling of downcoming waves around the crossover altitude [*Wang*, 1971; *Rodriguez and Gurnett*, 1971; *Gurnett et al.*, 1965; *Jones*, 1969]. The same phenomenon is observed in Figure 5 of *Rodriguez and Gurnett* [1971]. The light-ion trough seems to be a manifestation of the plasmapause. In this case, the decrease and smearing of the lower cutoff of the ELF hiss can provide a convenient way of determining the plasmapause location.

In what follows, we will be discussing mostly the properties and characteristics of the BLH. Examination of 270 occurrences (from spectrograms of the Ogo 4 broadband receivers) of hiss between September 1967 and March 1968 from Rosman, Quito, and Santiago revealed the following characteristics:

1. The BLH was seen in nearly all passes between 0600 and 2200 LT. It was not observed in the broadband data after ~2300 LT, although a few examples were found in the digital data (with smaller amplitude). Until a more extensive examination of the digital data is completed, no definitive conclusion can be drawn about the times of occurrence. At this point it can be said that the phenomenon is more common during local daytime.

2. The equatorial erosion is present in all records that cover the region around ±10° dipole latitude, and there is a marked symmetry in the phenomenon with respect to the magnetic equator.

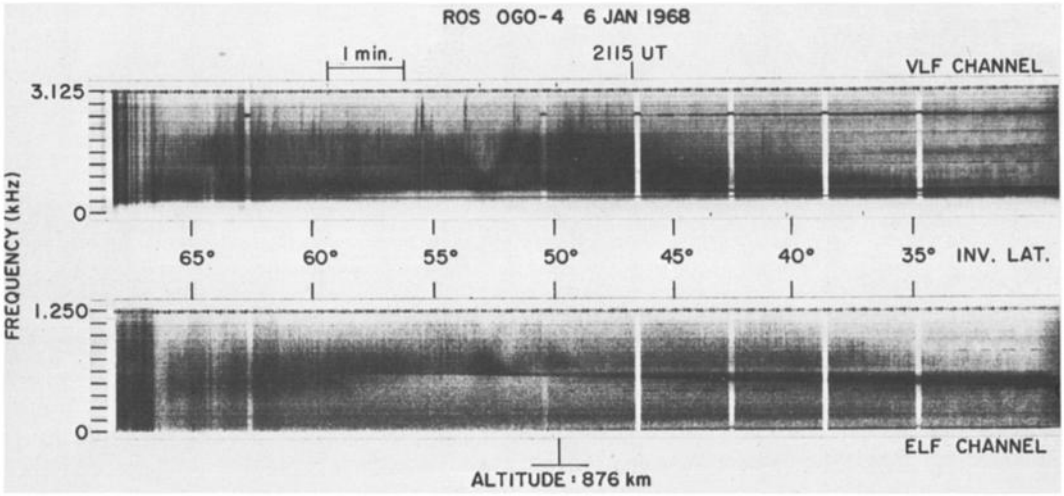

Fig. 3. Spectrograms similar to the ones in Figure 1 but recorded at higher latitude in Rosman, North Carolina. The BLH is again clearly visible up to ~55° invariant latitude, where the lower and upper cutoffs merge. The gradual disappearance of the lower cutoff of the hiss between 58° and 60° is probably due to the H^+ ion depletion reportedly observed at the plasmapause and could provide an additional way of determining its location. The altitude range in this pass is from 880 to 852 km.

3. The upper cutoff of the BLH in the vicinity of 600 Hz is nearly independent of satellite latitude above ~15°, and its sharpness shows variations from pass to pass. However, in ~40% of the passes examined, the sharpness is comparable to that in Figures 1 and 3. After prolonged periods of low magnetic activity, the upper cutoff frequency decreases to values as low as 420 Hz but recovers about one day after a sharp increase in activity (such as a sudden commencement). Figure 4 illustrates the change in upper cutoff after the quiet period from March 7 to 9, 1968. The spectrogram on the left (March 2) is typical of the period indicated from March 1 to 6 and has an upper cutoff of ~590 Hz. The spectrogram in the center (March 10) shows the lowering of the upper cutoff to ~470 Hz after three days of low activity ($Kp \leq 2$), and finally the one on the right shows the recovery of the upper cutoff to ~550 Hz one day after a sudden commencement. Similar decreases of the upper cutoff frequency have been observed during other calm periods (around November 18 and December 13, 1967).

Table 1 shows the average values of upper cutoff from Rosman and Santiago data during the months of January and March 1968 These data were selected from the cases of sharpest upper cutoff, excluding the periods of extremely low magnetic activity, such as the days preceding March 10 (see Figure 4). The table also shows the standard deviations (σ) and solar zenith angles (χ) for two approximately conjugate points (±35° dipole latitude). The months of January and March were chosen in order to provide a variety of ionospheric illumination conditions at both stations (as can be seen by the values of χ). The closeness between the resulting average values of upper cutoff frequency, plus the fact that near Santiago the geomagnetic field intensity is ~25% lower than near Rosman, indicates a lack of control of the upper cutoff frequency by the local ionosphere. Although the uncertainties involved in the determination of the cutoff frequency from the spectrograms are of the order of 3%, the average values for Rosman were consistently higher than those for Santiago (2.9% in January and 3.7% in March). This small difference may be attributed to the slight increase in upper cutoff with latitude, which will be discussed later.

As was mentioned in the introduction, some measurements of the amplitude of the signals were made by using data from the sweeping receivers of Ogo 4. These receivers cover three consecutive bands. Band 1, used here, has a bandwidth of 40 Hz and sweeps through 256 steps in the frequency range 0.15 to 1.54 kHz every 73.6 sec in the low bit rate (4 kb/sec). This information is recorded on magnetic tape aboard the satellite and can be transmitted to the ground on command from the telemetry stations, providing measurements along a full orbit (for more details on the experiment, see *Rorden et al.* [1966]). The quantity measured is the magnetic field B of the waves, and Figure 5 shows an example of such a measurement for the pass illustrated in Figure 1. The upper panel shows part of the spectrogram of Figure 1 containing the erosion on the northern-hemisphere side. The time scale here is expanded in relation to Figure 1, and the diagonal straight line across the spectrum represents the sweep of the band 1 sweeping receiver shown in the lower panel. The corresponding amplitude, in decibels below 1 γ, versus frequency shows the variation in signal strength across the two cutoffs (A and B) and the erosion (C). The spikes identified as interference appear usually at multiples of 400 Hz and are caused by inverters aboard the satellite. Along the sweep reproduced in the figure, the interference at 400 Hz is not seen. However, in the spectrogram, the lines at 400 Hz and 800 Hz can be easily identified. The noise level of the band 1 sweeping receiver varies from −60 db γ (2.5×10^{-8} γ^2/Hz) at 200 Hz to −97 db γ (5×10^{-12} γ^2/Hz) at 1500 Hz. The bump at 200 Hz seems to be real, since it is only observed at low latitudes, but it has not been interpreted yet.

In order to have a sample of how the amplitude of the noise varies with latitude, measurements were made along four orbits covering a range of +84° to −84° invariant latitude. Two of the passes were on February 18, and the other two on February 22, 1968. The result, plotted in units of γ^2/Hz versus invariant latitude, appears in Figures 6*a* and *b*. For each of the orbits, the amplitudes at three sets of frequencies were chosen for illustration: 600 Hz (immediately above the BLH) represented by dashed lines, 1000 Hz represented by continuous lines, and the frequency of maximum intensity

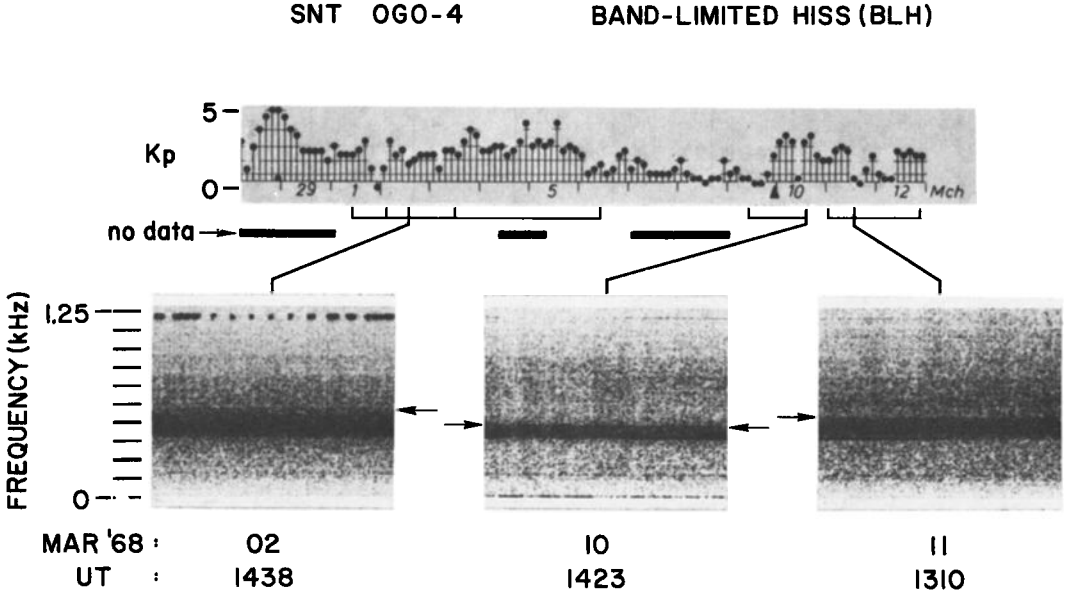

Fig. 4. Illustration of the decrease of the upper cutoff of the BLH after periods of low magnetic activity. The spectrograms (0–1.25 kHz) were made from broadband data recorded at Santiago between —29° and—35° dipole latitude during March 1968. In the spectrogram at the left, recorded during a moderately active day (March 2), the arrow indicates an upper cutoff of ~590 Hz. Comparable values of upper cutoff were also found on March 1, 3, and 6, as is indicated by the vertical bars below the Kp index scale. The spectrogram in the center (March 10) shows the decrease of the upper cutoff to ~470 Hz (also observed on March 9) after three days of low activity ($Kp \leq 2$). Notice the time lag of approximately one day between this spectrogram and the low Kp period. Finally, the spectrogram at right shows the recovery of the upper cutoff to ~550 Hz one day after a sudden commencement.

in the BLH represented by dash-dot lines. Three of the four passes in Figure 6 do not show recordings of amplitude for the whole range of latitudes covered by the satellite owing to changes in the mode of operation of the spacecraft.

The equatorial erosion is clearly visible and amounts to attenuations of 20 to 33 db (at 600 Hz) between two consecutive sweeps, corresponding to a change in latitude of about 4°. The maximum intensities at 600 Hz and 1000 Hz occur in the vicinity of ±60° invariant latitude and may be of the order of 10^{-4} γ^2/Hz. Beyond ±70°, the intensities decrease quite rapidly, and at approximately ±84° the background noise levels of the receiver are attained. In the range of 0 to 3 kHz and up to ~55° latitude, the BLH is the strongest signal observed.

In Figure 6*b* the maximum intensity of the BLH for the pass of February 22 in the southern hemisphere increases from —30° to —46° invariant latitude, where it peaks at $\sim 2 \times 10^{-4}$ γ^2/Hz. A sample of the range of intensities at 1.0 kHz and at the frequency of maximum amplitude in the BLH as a function of local

TABLE 1. Upper Cutoff Frequency of the BLH

Station	January 1968, 1330 LT				March 1968, 0800 LT			
	Avg. Upper Cutoff, Hz	σ, Hz	χ	No. Cases	Avg. Upper Cutoff, Hz	σ, Hz	χ	No. Cases
ROS	582	7	40°	13	591	12	63°	11
SNT	565	19	32°	13	569	15	70°	12

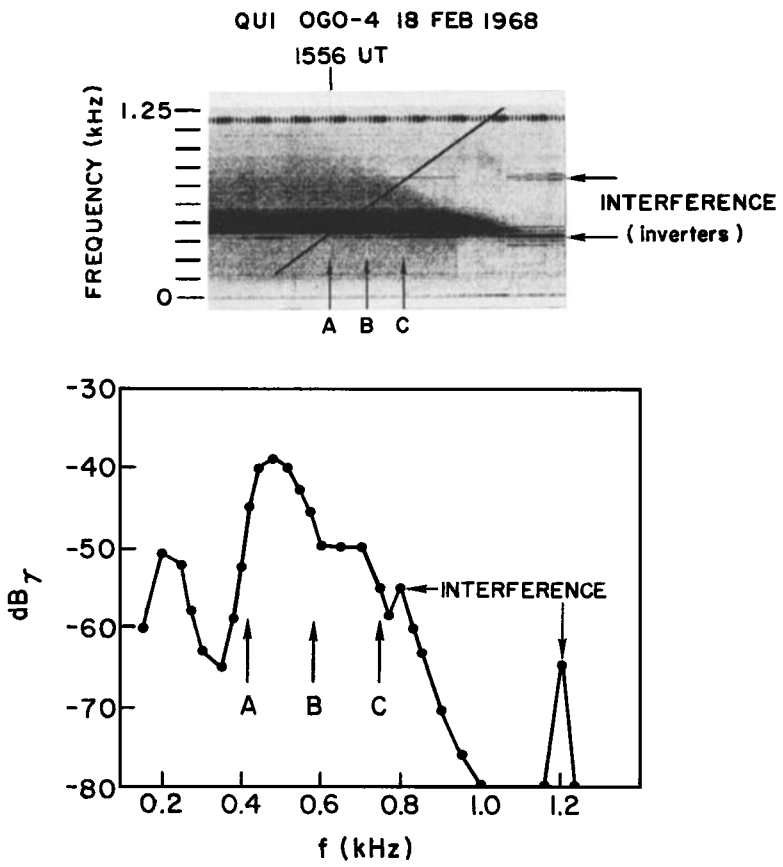

Fig. 5. Measurement of the hiss amplitude from the band 1 sweeping receiver on Ogo 4. The upper panel shows part of the spectrogram of Figure 1 containing the erosion on the northern hemisphere side. The time scale is expanded in relation to Figure 1, and the diagonal straight line across the spectrum represents the sweep of the band 1 receiver shown in the lower panel. This receiver sweeps a frequency range of 150 to 1540 Hz in 73.6 sec in the 4-kb/s mode. Its bandwidth is 40 Hz, and the amplitude variation of the magnetic field B of the waves is represented in decibels below 1 γ. The BLH is seen between cutoffs A and B, and cutoff C illustrates the effects of the erosion on the higher-frequency hiss. The interference at 1.2 kHz, clearly visible in the sweeping receiver data, is above the upper cutoff of the ELF broadband receiver and is not seen in the upper panel.

time was taken from 14 Ogo 4 passes between December 27, 1967, and April 15, 1968, and is shown in Figure 7. The four groups of values correspond to longitude ranges of $-40°$ to $-84°$ (values around 1000 LT and 2200 LT) and 115° to 128° (values around 0400 LT and 1600 LT). The four passes of Figures 6*a* and *b* are represented in the group around 1000 LT in Figure 7. The amplitudes at 1.0 kHz were taken in the same latitude range as the BLH in each pass. This range is limited by the merging of the increasing lower cutoff and the essentially steady upper cutoff, already illustrated in Figure 3. For a given satellite altitude, the lower cutoff frequency increases with latitude because of the corresponding increase in local magnetic field. (At higher altitudes, the lower cutoff should occur at lower frequencies, and the observation of the BLH would then extend to higher latitudes.)

Discussion

The symmetry of both the erosion and the upper cutoff in relation to the magnetic equator suggests that the BLH is generated near the equatorial plane. Since the above properties are

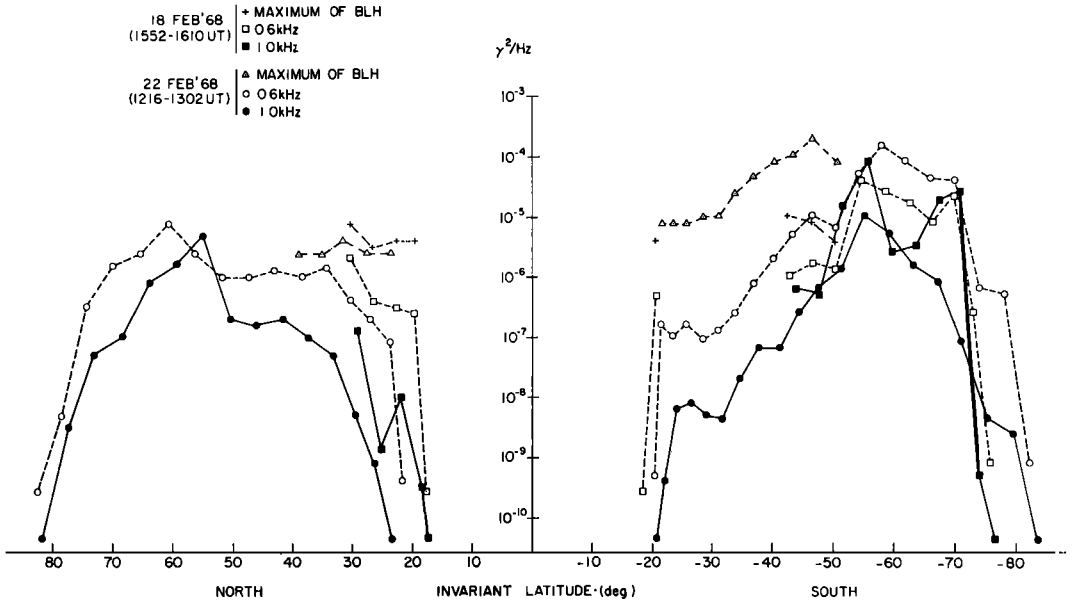

Fig. 6*a*. Intensity of the hiss in γ^2/Hz (which gives a measure of the power flux) versus invariant latitude for two satellite passes in February 1968. Continuous lines correspond to 1.0 kHz, dashed lines to 0.6 kHz, and dash-dot lines to the maximum intensity of the BLH. The gaps in the latitude coverage correspond to changes in the operating mode of the satellite. The erosion (at ~10° dipole latitude) corresponds to attenuation of 20 to 33 db between consecutive sweeps (~4° in latitude).

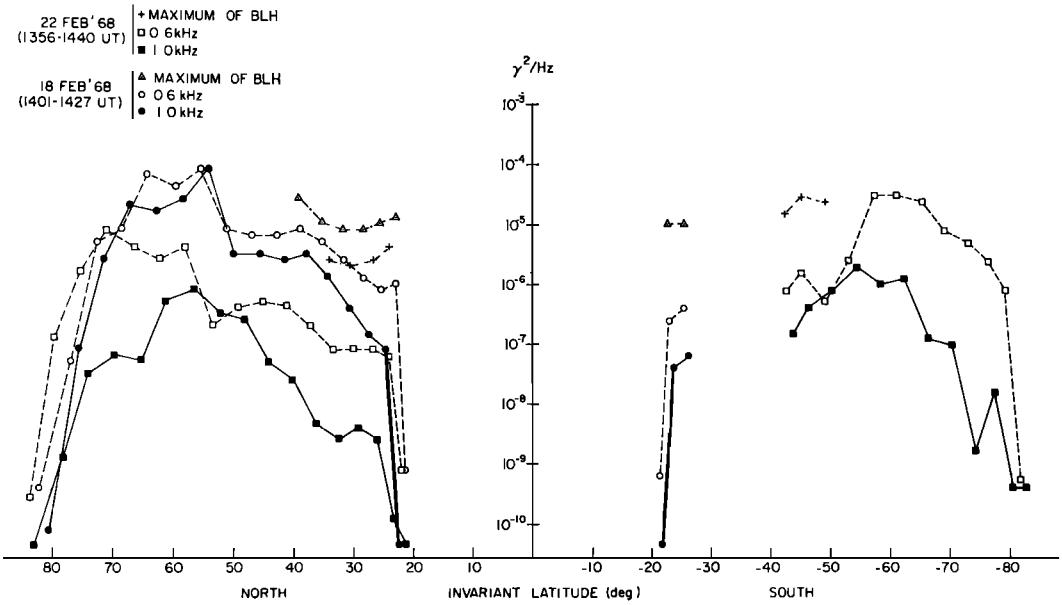

Fig. 6*b*. Similar to Figure 6*a* for two other passes on the same days. The hiss above the BLH peaks around ±60° invariant latitude, but the BLH itself seems to peak between −40° and −50° invariant latitude. In these four passes, the longitudes range from 40°W to 84°W, where the South Atlantic anomaly decreases the geomagnetic field in the southern hemisphere. This decreases the lower cutoff of the BLH and permits it to be seen up to ~−50° invariant latitude, whereas in the northern hemisphere the limit is ~40° invariant latitude.

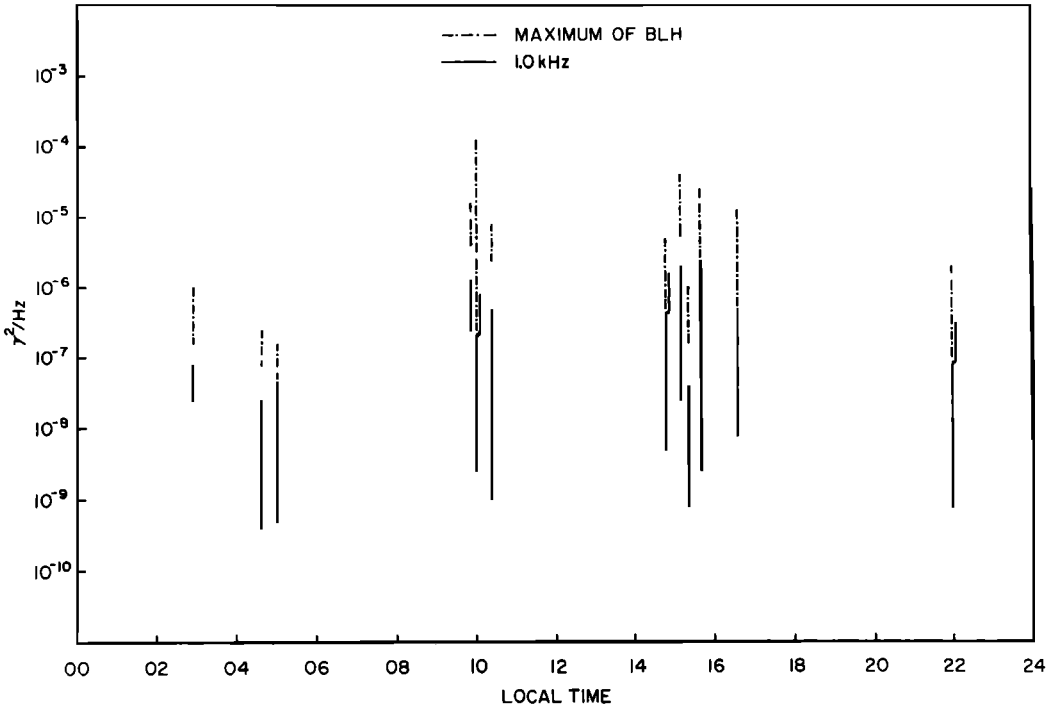

Fig. 7. Variation of hiss intensity with local time taken from sweeping receiver data corresponding to 14 Ogo 4 passes. The dash-dot lines correspond to the range of maximum intensity of the BLH (on both hemispheres), and the continuous lines represent the range of intensities at 1.0 kHz in the same latitudes where the BLH is seen. The BLH seems to peak around 1000 LT, where the four passes of Figures 6*a* and *b* are represented (each vertical line may contain data from more than one pass).

independent of local ionospheric conditions and satellite altitude, the source is expected to be quite far away from the Ogo 4 orbit.

A comparison with the observations and conclusions of previous papers on ELF hiss is restricted by the fact that most of them deal with high-latitude and/or high-altitude hiss. *Guthart et al.* [1968] interpreted the ELF hiss observed on Ogo 2 in terms of electrostatic waves. However, for an amplitude of -50 db γ (on a 40-Hz bandwidth), they need an electrostatic field of 40 v/m. On the other hand, our data indicate maximum intensities of 2×10^{-4} γ^2/Hz (-21 db γ on the same bandwidth; see Figure 6*a*), which would require electric fields of the order of 1000 v/m. Since electric fields of this order have not been directly observed, it seems appropriate to disregard that interpretation.

Gurnett and Burns [1968] report observations of ELF hiss for invariant latitudes larger than 35° and, from the description of the lower cutoff mechanism, conclude that the source of this kind of emission must be above 3000-km altitude. Although these authors did not mention the occurrence of the BLH, examination of their Figure 3 suggests its presence below ~600 Hz.

Using data from Ogo 3, *Russell et al.* [1969] studied the spacial extent of ELF noise and concluded that steady noise is most common on the dayside of the magnetosphere within $L = 6$. Their strongest amplitudes of steady signal (>4 volts in the 100-, 300-, or 800-Hz channels) showed a marked day-night asymmetry and were seen more frequently within $L = 5$, except between ~40 and 50° dipole latitude, where high rates of occurrence were found as far out as $L = 9$ or 10. These authors did not report measurements below $L = 2$. From the intensity of these signals, they concluded that 'on the dayside at low L values, the steady signals may be generated almost anywhere along a field line

up to 40° magnetic latitude, but at high L values on the dayside the signals must be generated in the range 40° to 50°.'

Reporting on data from Ogo 1, *Dunckel and Helliwell* [1969] observed ELF hiss of relatively constant intensity from 0.3 kHz to as high as 3 kHz, and from $L = 2.5$ up to the vicinity of the plasmapause ($L \doteq 4$). Maximum intensities in the vicinity of the equatorial plane occur between 06 and 16 LMT from $L = 2.5$ up to approximately $L = 4$, extending to $L = 5.5$ in the sector between 10 and 12 LMT. These maximum intensities are 16 db above 10^{-6} γ^2 Hz^{-1}. On the basis of the variation of upper cutoff with latitude, these authors concluded that the signals are generated close to the equatorial plane.

Studying the direction of the Poynting flux of ELF hiss with the Injun 5 satellite in the region 677- to 2528-km altitude and 35° to 75° invariant latitude (in the northern hemisphere), *Mosier* [1971] concluded that the hiss is generated outside the plasmasphere and propagates across the plasmapause at altitudes probably below ~2500 km. This conclusion is based on his observations of upgoing hiss at $L < 4$.

The possibilities offered by an equatorial source can be tested by using ray-tracing techniques. The results, as described in the following sections, are used to interpret the several characteristics of the BLH, the observations of ELF hiss outside the plasmapause between 40° and 50° reported by *Russell et al.* [1969], and also some of the Poynting-flux measurements of *Mosier* [1971]. In these ray tracings, the ionosphere model used is in diffusive equilibrium along magnetic field lines and describes quite well the daytime equatorial anomaly in the electron density.

Accessibility to low latitudes. Figures 8*a*, *b*, and *c* show ray paths for a frequency of 600 Hz starting at $L = 3$ in the equatorial plane for several values of the initial wave normal angle ψ_i. The wave normal angle ψ is measured from the magnetic field direction so that $|\psi| \leq 90°$, and is positive when the wave normal points toward lower L shells. The field line represented at $L = 4$ marks the position of a simulated plasmapause obtained by smoothly decreasing the electron density by a factor of 10 across a $\Delta L = 0.23$.

The lower hybrid resonance (LHR) frequency

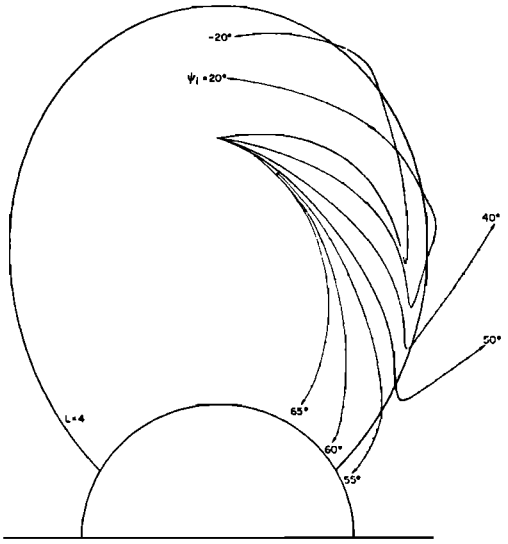

Fig. 8*a*. Ray paths of 600-Hz waves starting in the equatorial plane at $L = 3$ for different values of the initial wave normal angle ψ_i (the wave normal angle is counted from the geomagnetic field direction and is positive when the wave normal points toward lower L shells) obtained by ray tracings. The field line at $L = 4$ marks the position of a simulated plasmapause obtained by smoothly decreasing the electron density by a factor of 10 across a $\Delta L \doteq 0.23$. The rays corresponding to ψ_i between 40° and 50° escape from the plasmasphere.

at $L = 3$ in the equatorial plane is ~750 Hz, and so the refractive index surface at 600 Hz is closed. After the waves leave the equatorial plane, the behavior of the wave normal angle depends on its initial value, in a manner consistent with that shown by *Thorne and Kennel* [1967]. In the present case, if $\psi_i \leq 50°$ (Figure 8*a*), ψ decreases continuously until it reaches −90°, at which point the rays are refracted upward.

For $\psi_i > 55°$, ψ first decreases, reaches a minimum value, and then increases again. In addition, with increasing ψ_i, the minimum value of ψ also increases, and the point at which this minimum occurs approaches the equator.

If $\psi_i \geq 70°$, the minimum wave normal angle is reached so close to the equator that ψ may be able to increase up to +90°, when the rays will be refracted inward, producing the kind of ray paths illustrated in Figure 8*b*. For these ray paths, each time the equatorial plane is crossed the wave normal moves closer to the

geomagnetic field direction (ψ decreases) and it may happen that, after a few zig-zags, the equatorial value of ψ will be so low as to cause the next refraction to be upward (as for ψ_i = 70° in Figure 8*b* after the first refraction). If the initial wave normal angle is large enough ($\psi_i > 75°$ in the figure), the rays will bounce back and forth across the equatorial plane on their way down, and these are the only rays capable of reaching latitudes less than ~30° (Figures 8*b* and *c*; the wave normals corresponding to ψ_i = 70° and 75° are indicated by arrows in Figure 8*b*). Although the initial wave normal angles have to be large, the wave normal angles at low altitudes will be influenced by the ionospheric density gradients and can assume different values.

Erosion. In order to understand the distribution of energy around the equator, ray tracings were made at intervals $\Delta\psi_i$ = 0.1° from 85.5° up to 89°. Two frequencies were used, 500 and 600 Hz, and the results are plotted in Figure 9 as latitudes of arrival (at 700-km altitude) versus initial wave normal angles. The points distribute themselves in two groups on both sides of the equator, and for a uniform increase in ψ_i there are sudden jumps from one hemisphere to the other. This defocusing effect produces an attenuation of signals across the equator, as observed in the satellite recordings. It is possible to make a rough estimate of the relative intensity of the signals by assuming that the intensity is inversely proportional to the spacing between adjacent points. For the distribution of points in Figure 9, the result is shown in Figure 10, where intensities (on an arbitrary linear scale) are plotted versus the absolute value of dipole latitude. The irregularities in the resulting curves are due to the utilization of the discrete (and small) number of points from Figure 9. If a larger number of points had been used, the curves of Figure 10 would be smoother and their slope would be steeper. Nonetheless, from ~10° to ~17°, the intensity for 500 Hz is consistently higher than the one for 600 Hz, and a receiver with a constant threshold sensitivity in this range of frequencies

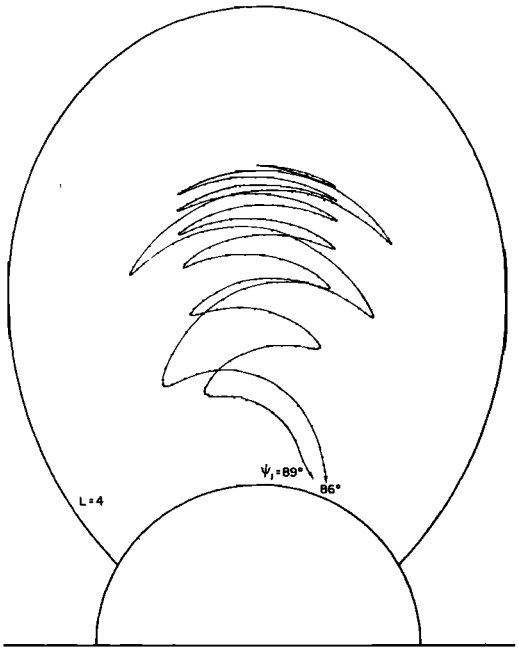

Fig. 8*c*. Similar to Figures 8*a* and *b*, but for ψ_i = 86° and 89°.

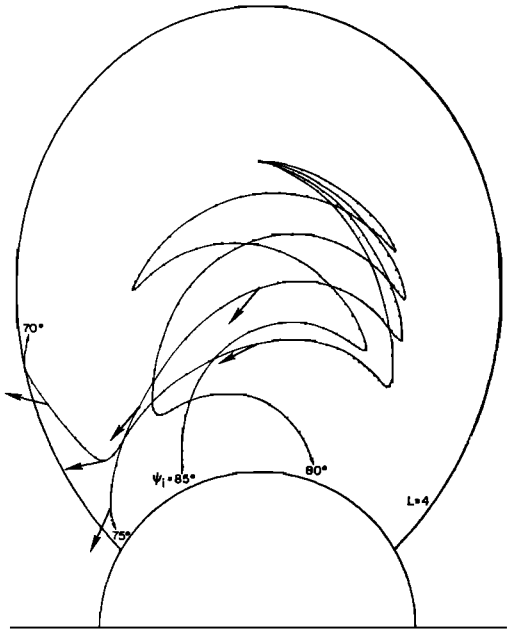

Fig. 8*b*. Similar to Figure 8*a*, but with initial wave normal angles increasing from 70° to 85°. The arrows represent wave normals in the ray paths corresponding to ψ_i = 70° and 75°, where the decrease in wave normal angle at the second equator crossing can be seen. This decrease may prevent the corresponding ray from attaining Ogo 4 altitudes (as for ψ_i = 70°). For large enough ψ_i (>75° in this case), the rays will reach the ionosphere following 'zig-zag' paths, and these are the only ones that can reach lower latitudes.

(as in Ogo 4) would observe an erosion as in Figure 1.

Upper cutoff. Another characteristic of the BLH reported here is the apparent constancy of the upper cutoff frequency observed in spectrograms from the broadband receivers. However, when examining the amplitude data from the sweeping receivers, one sometimes notices a slight displacement (variable from pass to pass) of the upper cutoff toward higher frequencies with increasing latitudes. This displacement is, however, much smaller than the corresponding variation of the lower cutoff. To illustrate that displacement, the output of the band 1 sweeping receiver corresponding to parts of three Ogo 4 passes is shown in Figure 11. For each of the passes, the consecutive sweeps are shown closely spaced in order to enhance their differences. Latitudes increase toward the bottom of the figure, and the mentioned displacement is quite noticeable, mainly in the pass at 2200 LT, February 22. The sharpness of the upper cutoff is also variable, and for the pass of December 27 it has a slope ranging from 8 to 15 db/100 Hz. In the sample of 14 passes examined, this slope varied between 8 and 20 db/100 Hz, whereas the lower cutoff was usually steeper (between 15 and 50 db/100 Hz).

The upper cutoff of the BLH can also be understood if the source is in the equatorial plane. The ray tracings of Figure 8, starting at $L = 3$, were intended to illustrate the general behavior of rays inside the plasmasphere, and they indicate the need for large initial wave normal angles in order to reach latitudes less than ~30° at low altitudes. If the source altitude is varied, however, the behavior of rays will not differ much from those illustrated. In the discussion of the erosion effect, it was mentioned that the refractive index surfaces corresponding to the waves propagating toward lower L shells in Figure 8 were closed. (The LHR frequency at $L = 3$ in the equatorial plane is ~750 Hz.) It is necessary that the surfaces be closed in order to produce the sudden refraction characteristic of the zig-zag ray paths; otherwise the wave normal angle could never attain 90°. When the frequency is increased past the equatorial or initial value of the LHR, the refractive index surfaces become open in that region, but it is still possible to generate zig-zag ray paths if the initial ratio (f/f_{LHR}) is not much greater than unity. This is so because the rays will be moving away from the equatorial plane approximately along magnetic field lines, and the local magnetic field

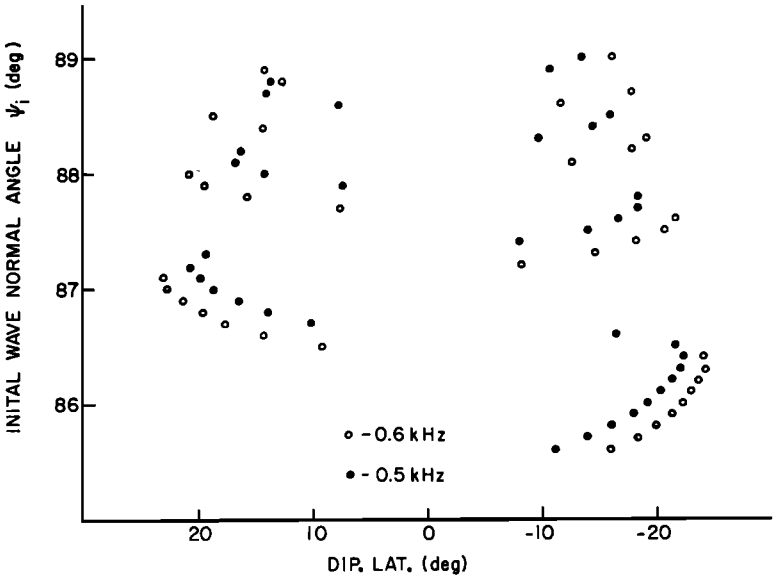

Fig. 9. Latitudes of arrival of rays, as in Figure 8, as a function of initial wave normal angle ψ_i. Two frequencies were used (500 and 600 Hz), and ψ_i was varied in steps of 0.1° from 85.5° up to 89°. The points distribute themselves in two groups on both sides of the equator, which creates a defocusing effect, resulting in the observed erosion (see Figure 10).

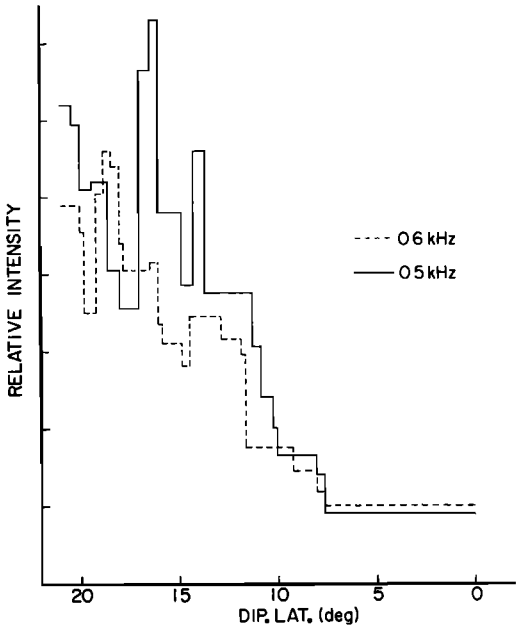

Fig. 10. Relative intensities (on a linear scale) obtained from the distribution of points in Figure 9 versus the modulus of dipole latitude. The intensities are obtained by assuming that they are inversely proportional to the spacing between adjacent points. With a larger number of points, the curves would be smoother and would have a steeper slope. Nonetheless, from ~10° to 17°, the intensity for 500 Hz is consistently higher than the intensity for 600 Hz, and a receiver with a more or less constant threshold sensitivity in this range of frequencies (as in Ogo 4) would observe an erosion as in Figure 1.

intensity will increase quite rapidly (and the f_{LHR} with it). Soon a point will be reached where the local f_{LHR} becomes larger than the wave frequency, and the refractive index surfaces will be closed again. From the results of ray tracings with frequencies that obey the above condition, it was found that when the frequency is increased:

1. There is an increase in the minimum value of initial wave normal angle (ψ_i) necessary to generate a zig-zag ray path down to Ogo 4 altitudes.
2. For this minimum value of ψ_i, the latitude of arrival of the rays also increases slightly.

However, as the frequency is increased above the LHR frequency, the resonance angle (where the refractive index $\mu \to \infty$) decreases. Actually, when ψ_i becomes larger than ψ_m (defined as the value of ψ for which the product $\mu \cos \psi$ is minimum), the rays begin to move toward larger L shells and are not able to reach low altitudes. If the source of the hiss is in the equatorial plane, a low-altitude satellite like Ogo 4 will observe an upper cutoff (somewhat above the LHR frequency at the generating region) that should increase slightly with latitude. In the examples of Figure 8, with the origin at $L = 3$, this upper cutoff happens above 1 kHz. In order to obtain a cutoff close to 600 Hz, the source has to be moved to a higher altitude. If the source is moved to $L = 4$, the equatorial value of the LHR frequency is reduced to approximately 320 Hz. Some rays were actually traced for a frequency of 600 Hz starting at that altitude, and it was found impossible to make any rays arrive at latitudes lower than 50° and low altitudes. A source close to $L = 4$ would therefore produce a hiss band with characteristics similar to the observed BLH, and its upper cutoff

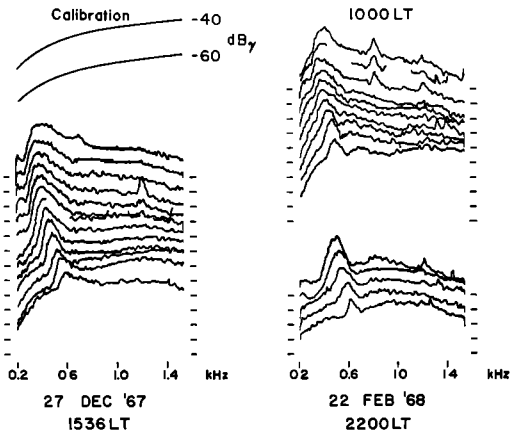

Fig. 11. Reproduction of band 1 sweeping receiver outputs for three Ogo 4 passes where the BLH can be easily recognized as the large amplitude bump below ~600 Hz. Subsequent sweeps were reproduced closely spaced in order to enhance variations in the shape of the BLH. Latitudes increase toward the bottom of the page, and one can see a slight displacement of the upper cutoff toward higher frequencies with increasing latitudes. At the same time, the lower cutoff increases by a much larger amount. The slope of the upper cutoff is also somewhat variable. The calibration curves on the upper left correspond to −40 and −60 db γ.

would be essentially independent of the magnetic latitude and local conditions at the satellite.

The observed decrease of the upper cutoff of the BLH shown in Figure 4 would also be understood, in the context of the present interpretation, as an outward drift of the generation region during periods of very low magnetic activity.

Leakage from plasmasphere. Transmission of rays to regions outside the plasmasphere can occur for initial wave normal angles ψ_i varying from 40° to 50° as shown in Figure 8*a*. This result can be used to explain the observations of *Russell et al.* [1969] of daytime occurrences of 'steady noise' outside the plasmasphere between 40° and 50° dipole latitude. The rays with $\psi_i < 40°$ are refracted back to the plasmasphere by the steep density gradient that constitutes the plasmapause and are trapped inside. The ray path corresponding to $\psi_i = 55°$ is bent downward, also by the gradient at the plasmapause, and if $\psi_i > 55°$ the rays are confined within the plasmasphere. Even when the rays were started at higher altitudes, as was mentioned in the preceding section, the leakage to the outside across the plasmapause could still be observed around ~45° dipole latitude.

Direction of Poynting flux. In his study of the direction of Poynting flux using data from the Injun 5 satellite, *Mosier* [1971] reported the occurrence of downgoing ELF hiss over a range of invariant latitudes from ~40° to more than 70° (across the plasmapause). The highest invariant latitude at which he observed the Poynting flux of the hiss directed upward was about 60° (approximately the plasmapause location), and during the daytime these occurrences were always above 1500 km. Again, from the ray paths in Figure 8*a*, it can be concluded that below ~3000 km and outside the plasmasphere the rays are always propagating downward, but in the plasmasphere rays propagating both downward and upward are encountered (Figure 8*b*). If $70° \leq \psi_i \leq 75°$, for example, some rays were traced that refracted upward at altitudes as low as 2500 km. With a nighttime density model, this altitude was easily lowered to 1200 km, using frequencies as high as 900 Hz. As was mentioned before, the wave normal angles at low altitudes are sensitive to density gradients and are therefore dependent on the model used.

GENERATION MECHANISM

The characteristics of the BLH presented and discussed in preceding sections suggest a source location near the equatorial plane in the vicinity of $L = 4$ and the necessity of large initial wave normal angles. In this section, we discuss briefly two generation mechanisms and make a simple estimate of the energy levels and particle numbers that can reproduce the measured values of hiss intensity.

The two most popular radiation mechanisms to explain VLF and ELF emissions from the magnetosphere are Cerenkov and Doppler-shifted cyclotron (DSC) radiation from electrons trapped in the earth's magnetic field [*Ellis*, 1957; *Gallet*, 1959; *Gallet and Helliwell*, 1959; *Dowden*, 1962, 1963; *McKenzie*, 1963, 1967; *Bell and Buneman*, 1964; *Brice*, 1964; *Liemohn*, 1965; *Kennel*, 1966; *Kennel and Thorne*, 1967; *Helliwell*, 1967; *Mansfield*, 1967; *Jørgensen*, 1968; *Melrose*, 1968; *Russell and Thorne*, 1970; *Trulsen and Fejer*, 1970]. Without going into details on the radiation processes (see above references), the conditions for Cerenkov (or Landau) and DSC resonance between waves and electrons can be described by the following expressions [*Liemohn*, 1965]:

$$\mu \cos \psi = 1/\beta_\parallel$$

for Cerenkov (or Landau) resonance, and

$$\mu \cos \psi = 1/\beta_\parallel[1 - m(f_H/\gamma f)]$$

for DSC resonance. In these expressions, μ is the wave refractive index, ψ is the wave normal angle of the emitted radiation, $\beta_\parallel$ is the parallel component of the normalized particle velocity ($\beta = v/c$), f_H is the electron gyrofrequency, f is the frequency of the radiation, $\gamma = (1 - \beta^2)^{-1/2}$ accounts for relativistic effects, and m is an integer (the case $m = 0$ corresponds to the Cerenkov emission). When $f_H/\gamma f > 1$, the emission is either in the forward or the backward hemisphere depending on the sign of the integer m. If $m \leq 0$, the emission is in the forward hemisphere ($\cos \psi$ and $\beta_\parallel$ of same sign), and if $m > 0$ the emission is in the backward hemisphere ($\cos \psi$ and $\beta_\parallel$ of opposite signs), as is illustrated in Figure 12.

For the range of frequencies encountered in

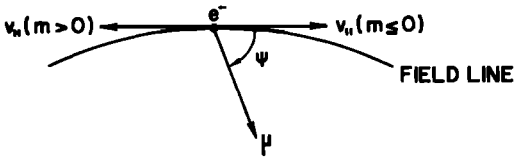

Fig. 12. Relative positions of the parallel component of the emitting electron velocity and the wave normal in a magnetic meridian plane for the case of Cerenkov or Landau resonance ($m = 0$) and Doppler-shifted cyclotron resonances ($m \leqq 0$).

the BLH and the source location discussed here (near $L = 4$), the product $\mu \cos \psi$ can be as low as 18, owing to the large wave normal angles involved. If one considers the Cerenkov process, the above expression for the condition of resonance indicates electron energies of the order of 1 kev. On the other hand, the DSC mechanism will involve electron energies near 1 Mev.

Expressions for computing the power emitted by a single electron on the Cerenkov and DSC mechanisms can be found elsewhere [*Mansfield*, 1967; *Melrose*, 1968; *Trulsen and Fejer*, 1970]. The quantity computed is the power radiated per frequency interval (dP/df) as a function of the particle velocity components $v_\parallel$ and $v_\perp$, respectively, parallel and perpendicular to the earth's magnetic field, and the characteristics of the medium. For a frequency of 400 Hz and a wave normal $\psi_i = 87°$ in the equatorial plane at $L = 3.8$, we found:

For the Cerenkov mechanism (electron energy, 0.56 kev):

$$dP/df \doteq 4 \times 10^{-34} \text{ watt/Hz}$$

For the DSC mechanism (electron energy, 780 kev):

$$dP/df \doteq 1 \times 10^{-34} \text{ watt/Hz}$$

The emitted power per electron is of the same order of magnitude in both mechanisms. *Frank* [1968] indicates omnidirectional electron fluxes (0.3 to 3 kev) of 2×10^9 el/cm^2 sec around $L = 4$. For the high-energy particles ($E > 500$ kev), *Vernov et al.* [1969] indicate intensities of about 6×10^6 el/cm^2 sec. Comparing these two intensities and considering the differences in particle velocities, the number density of the low-energy electrons will be from 10^4 to 3×10^4 times larger than that of the high-energy electrons.

Taking the above value of dP/df obtained for the Cerenkov emission mechanism, the power flux emitted by a single electron can be computed. By comparing this result with the power fluxes measured by Ogo 4, the order of magnitude of the number of emitting electrons can be estimated. In a frequency interval Δf, each electron radiates through an annulus subtending a wave normal angle $\Delta\psi$ around ψ_i, but only a small segment of this annulus, pointing toward the earth, will contribute to the power received by the satellite. Taking for instance a segment of 2° (that is, considering wave normals slightly off the meridian plane) and making the conservative assumption that only rays starting inside this segment will propagate down to Ogo 4 altitudes, it is possible to estimate the area ΔA illuminated by this segment for a given Δf and the corresponding $\Delta\psi$. (The rays off the meridian plane were traced utilizing a three-dimensional computer ray-tracing program developed by F. Walter.) Taking for Δf the bandwidth of the band 1 sweeping receiver (40 Hz), the area ΔA is found to be

$$\Delta A \doteq 3.6 \times 10^{11} \text{ m}^2$$

which corresponds to an emitted power flux per electron (S_E) of

$$S_E \doteq 2.5 \times 10^{-46} \text{ watt/m}^2$$

From the intensity found in the BLH at low latitudes ($\sim 5 \times 10^{-6}$ γ^2/Hz, Figures 6*a* and *b*) and assuming a value of 50 for the refractive index, the measured power flux on the same 40-Hz bandwidth is found to be of the order of

$$S_M \doteq 4 \times 10^{-10} \text{ watt/m}^2$$

Assuming that the hiss is generated incoherently, the ratio of these power fluxes gives the number of emitting electrons:

$$N = (S_M/S_E) \doteq 1.6 \times 10^{36} \text{ electrons}$$

It is easily verified that this is an excessively large number, since even for a density of 10 el/cm^{-3} [cf. *Schield and Frank*, 1970], it corresponds to a volume greater than 10,000 magnetospheres. Therefore, some form of coherency in the emission generation, or wave growth, is

needed to produce the observed power fluxes. It can easily be verified that similar requirements also hold for the Doppler-shifted cyclotron generation. However, a detailed study of the possibilities of wave growth in the DSC mechanism is outside the scope of this work. An excellent treatment of the problem is given by *Russell and Thorne* [1970], although these authors emphasize small wave normal angles and frequencies higher than in the BLH. A greater knowledge of the low-energy electron fluxes in the vicinities of the plasmapause and their drifts with magnetic activity could provide a test for comparison of the two emission mechanisms.

SUMMARY

Analysis of ELF and VLF data from the Stanford University experiment aboard Ogo 4 from September 1967 to April 1968 revealed some not yet identified features of a known ELF hiss band. The principal features of this band (BLH) are listed below.

1. The lower cutoff frequency increases with latitude, typical of downward-propagating hiss, and is attributed to the two-ion cutoff in the dispersion relation [*Gurnett and Burns*, 1968].

2. The upper cutoff frequency is close to 600 Hz and seems to be essentially independent of latitude above ~15° or 20° (Figure 1), although sometimes it can show a slight increase toward higher latitudes (see Figure 11). After a prolonged period of low magnetic activity ($Kp \leq 2$), the upper cutoff frequency may decrease to approximately 420 Hz but recovers about one day after a sharp increase in Kp or a sudden commencement (Figure 4). (The data examined did not include any period of intense magnetic activity, $Kp > 6$.)

3. The upper cutoff decreases in frequency toward the equator near 10° dipole latitude (equatorial erosion; Figure 1). The attenuation rates in the region of erosion are in the range of 20 to 33 db at 600 Hz for a latitude change of ~4° (Figures 6*a* and *b*).

4. The latitude of occurrence extends from ~10° up to ~55° dipole latitude, where the essentially constant upper cutoff and the increasing lower cutoff merge (cf. Figure 3). This limiting latitude depends on the local magnetic field intensity and the satellite altitude.

5. The most frequent times of occurrence lie between 0600 and 2200 LT (when it showed up in almost every Ogo 4 pass), although some occurrences have been found between 0200 and 0500 LT (with less intensity).

6. The local ionosphere has no apparent effect upon the upper cutoff frequency.

Between the latitudes of ~10° and ~55°, the BLH contains the strongest signals in the frequency range of 0 to 3 kHz. Its intensity peaks between 40° and 50° dipole latitude and may reach 2×10^{-4} γ^2/Hz during daytime (~1000 LT; see Figure 6*b*). The decrease and smearing of the lower cutoff of the background hiss, observed above 58° invariant latitude, is an indication of the light ion trough.

The characteristics of the BLH suggest a source location in the equatorial region near $L = 4$ and the need for large initial wave normal angles. This source location provides an explanation of:

1. The presence of the BLH at low latitudes and the equatorial erosion.
2. The nearly constant upper cutoff of the BLH.
3. The daytime observation of hiss outside the plasmapause between 40° and 50° latitude reported by *Russell et al.* [1969].
4. Some observations of Poynting flux direction reported by *Mosier* [1971].

The Cerenkov and Doppler-shifted cyclotron (DSC) generation mechanisms from trapped electrons are briefly examined as possible sources of the BLH. For the frequency range in question, the electron resonance energies are of the order of 1 kev for the Cerenkov emission and close to 1 Mev for the DSC emission, and the power radiated by a single electron is comparable in both mechanisms. In either case, however, some degree of coherency or amplification is necessary to explain the observed power fluxes. At this point, it is not clear which one of the two emission processes is responsible for the BLH, and a more detailed study of the low-energy electron drifts with magnetic activity could provide an answer.

Acknowledgments. The authors wish to thank R. A. Helliwell, J. Katsufrakis, T. Bell, and C.

Park for helpful discussions related to the paper. The use of a tridimensional ray-tracing program developed by F. Walter is also acknowledged.

The research for this paper was supported by the National Aeronautics and Space Administration under contract NAS 5-3093, grant NGR-288, and grant NgL-008. Computer facilities were sponsored in part by the Office of Computer Sciences of the National Science Foundation under grant NSF GP-948.

* * *

The Editor wishes to thank D. A. Gurnett, C. T. Russell, and F. L. Scarf for their assistance in evaluating this paper.

REFERENCES

Bell, T. F., and O. Buneman, Plasma instability in the whistler mode caused by a gyrating electron stream, *Phys. Rev., 5A,* A1300–A1302, 1964.

Brice, N. M., Fundamentals of very low frequency emission generation mechanisms, *J. Geophys. Res., 69,* 4515–4522, 1964.

Dowden, R. L., Theory of generation of exospheric very low frequency noise (hiss), *J. Geophys. Res., 67,* 2223–2230, 1962.

Dowden, R. L., Doppler shifted cyclotron generation of exospheric very low frequency noise (hiss), *Planet. Space Sci., 11,* 361–369, 1963.

Dunckel, N., and R. A. Helliwell, Whistler-mode emissions on the Ogo 1 satellite, *J. Geophys. Res., 74,* 6371–6385, 1969.

Ellis, G. R. A., Low frequency radio emission from aurorae, *J. Atmos. Terr. Phys., 10,* 302–306, 1957.

Frank, L. A., On the distribution of low energy protons and electrons in the earth's magnetosphere, *Earth's Particles and Fields,* edited by B. M. McCormac, Reinhold, New York, 1968.

Gallet, R. M., The very low frequency emissions generated in the earth's exosphere, *Proc. IRE, 47,* 211–231, 1959.

Gallet, R. M., and R. A. Helliwell, Origin of very low frequency emissions, *J. Res. NBS, 63D,* 21–27, July-August 1959.

Gurnett, D. A., and B. Burns, The low frequency cutoff of ELF emissions, *J. Geophys. Res., 73,* 7437–7445, 1968.

Gurnett, D. A., S. D. Shawhan, N. M. Brice, and R. L. Smith, Ion cyclotron whistlers, *J. Geophys. Res., 70,* 1665–1688, 1965.

Guthart, H., T. L. Crystal, B. P. Ficklin, W. E. Blair, and T. J. Yung, Proton gyrofrequency band emissions observed aboard Ogo 2, *J. Geophys. Res., 73,* 3592–3596, 1968.

Helliwell, R. A., A theory of discrete VLF emissions from the magnetosphere, *J. Geophys. Res., 72,* 4773–4790, 1967.

Jones, D., The effect of the latitudinal variation of the terrestrial magnetic field strength on ion cyclotron whistlers, *J. Atmos. Terr. Phys., 31,* 971–981, 1969.

Jørgensen, T. S., Interpretation of auroral hiss measured on Ogo 2 and at Byrd station in terms of incoherent Cerenkov radiation, *J. Geophys. Res., 73,* 1055–1069, 1968.

Kennel, C. F., Low-frequency whistler mode, *Phys. Fluids, 9,* 2190–2202, 1966.

Kennel, C. F., and R. M. Thorne, Unstable growth of unducted whistlers propagating at an angle to the geomagnetic field, *J. Geophys. Res., 72,* 871–878, 1967.

Liemohn, H. B., Radiation from electrons in magnetoplasma, *Radio Sci., 69D,* 741–766, May 1965.

Mansfield, V. N., Cerenkov and cyclotron radiation as VLF emission sources, *Astrophys. J., 147,* 672, 1967.

McKenzie, J. F., Cerenkov radiation in a magneto-ionic medium (with application to the generation of low frequency electromagnetic radiation in the exosphere by the passage of charged corpuscular streams), *Phil. Trans. Roy. Soc. London, A255,* 585–606, 1963.

McKenzie, J. F., Radiation losses from a test particle in a plasma, *Phys. Fluids, 10,* 2680–2694, 1967.

Melrose, D. B., The emissivity in the magneto-ionic modes, *Astrophys. J., 154,* 803–806, 1968.

Mosier, S. R., Poynting flux studies of hiss with the Injun 5 satellite, *J. Geophys. Res., 76,* 1713–1728, 1971.

Rodriguez, P., and D. A. Gurnett, An experimental study of very-low-frequency mode coupling and polarization reversal, *J. Geophys. Res., 76,* 960–971, 1971.

Rorden, L. H., L. E. Orsak, B. P. Ficklin, and R. H. Stehle, Instruments for the Stanford University/Stanford Research Institute VLF experiment (4917) on the Eogo satellite, *Instr. Rep.,* Stanford Res., Inst., Menlo Park, Calif., 1966.

Russell, C. T., R. E. Holzer, and E. J. Smith, Ogo 3 observations of ELF noise in the magnetosphere, 1, Spatial extent and frequency of occurrence, *J. Geophys. Res., 74,* 755–777, 1969.

Russell, C. T., and R. M. Thorne, On the structure of the inner magnetosphere, in *Cosmic Electrodynamics,* vol. 1, 67–89, D. Reidel, Dordrecht, Netherlands, 1970.

Scarabucci, R. R., Satellite observations of equatorial phenomena and defocusing of VLF electromagnetic waves, *J. Geophys. Res., 75,* 69–84, 1970.

Schield, M. A., and L. A. Frank, Electron observations between the inner edge of the plasma sheet and the plasmasphere, *J. Geophys. Res., 75,* 5401–5414, 1970.

Taylor, H. A., H. C. Brinton, D. L. Carpenter, F. M. Bonner, and R. L. Heyborne, Ion depletion in the high-latitude exosphere: Simultaneous Ogo 2 observations of the light ion trough and the VLF cutoff, *J. Geophys. Res., 74,* 3517–3528, 1969.

Taylor, W. W. L., and D. A. Gurnett, Morphology of VLF emissions observed with the Injun 3 satellite, *J. Geophys. Res., 73,* 5615–5626, 1968.

Thorne, R. M., and C. F. Kennel, Quasi-trapped

VLF propagation in the outer magnetosphere, *J. Geophys. Res., 72,* 857–870, 1967.
Trulsen, J., and J. A. Fejer, Radiation from a charged particle in a magnetoplasma, *J. Plasma Phys., 4,* 825–841, 1970.
Vernov, S. N., E. V. Gortchakov, S. N. Kuznetsov, Yu. I. Logachev, E. N. Sosnovets, and V. G. Stolpovsky, Particle fluxes in the outer geomagnetic field, *Rev. Geophys., 7,* 257–280, 1969.
Wang, Ting-i, Intermode coupling at ion whistler frequencies in a stratified collisionless ionosphere, *J. Geophys. Res., 76,* 947–959, 1971.

(Received August 11, 1971;
accepted November 30, 1971.)